THERMAL STRESSES IN CONCRETE BRIDGE SUPERSTRUCTURES UNDER SUMMER CONDITIONS

M. Radolli and R. Green, Department of Civil Engineering,
University of Waterloo

Current design practice for deep concrete bridge superstructures generally ignores the influence of the diurnal heating cycle on the flexural response of members and, instead, considers mean temperature effects. A 1-dimensional heat-flow analysis is used to study the flexural deformations and stresses that are developed in deep concrete sections as a result of a typical summer heating cycle. Both nonlinear temperature and stress distributions are observed, and nonlinearity increases with member depth. An analysis of 2 typical continuous concrete structures indicates stresses exceeding those associated with live load and amounting to 40 percent of the allowable area possible for concrete structures having a depth of more than 4 ft (1.22 m).

•BRIDGE superstructures are affected by daily and seasonal temperature changes. These temperature changes cause longitudinal movement. In design of concrete superstructures, this movement together with creep and shrinkage is provided for with expansion joints (1). Little or no reference is made in design specifications to the effects resulting from temperature gradients through the depth of the bridge (2). The stresses resulting from these gradients appear to be closely related to the depth of the structure.

Concrete structures are being used more frequently for medium- and long-span bridges. The depth of these structures increases even though depth-to-span ratios may be nearly constant. Because of the increase in depth and because of the poor heat conductivity of concrete, temperature differentials between both upper and lower surfaces and interior and exterior of these deeper structures become considerably greater than those previously experienced for simple short-span structures.

Concern for predicting stresses that develop as a consequence of temperature gradients in deeper concrete structures is based on serviceability rather than strength. High local stresses can be induced during a temperature cycle of 12 h. For example, in a concrete structure, a free strain of 240 microstrains is possible on a hot summer day and easily might occur more than a thousand times during the life of the structure. This compares with the total shrinkage strain of 200 microstrains that is suggested in specifications (2). Local stresses caused by thermally induced strains frequently do not have the same sign as stresses induced by combinations of dead load, live load, and prestress (3).

Reynolds and Emanuel (1) have provided design engineers with a discussion of the most recent knowledge on thermal response of bridge structures. They have pointed out the need for further study of the prediction of thermal stresses. This paper discusses the form of both temperature gradients and stresses induced by these gradients in simple and continuous structures. Vertical temperature gradients can be nonlinear and result in nonlinear stress distributions. Such stress distributions frequently are not discussed in elementary texts. Analyses of several sections subjected to summer solar heating were carried out, and stresses exceeding live load stresses were predicted in a number of cases. A discussion of various field observations of bridge movements caused by temperature effects also is included in this paper.

Publication of this paper sponsored by Committee on Concrete Bridges.

TYPES OF THERMAL STRESS

The behavior of a structure as a result of the application of heat is different from its behavior caused by strain accompanied by stress, which results from load application. Strains do not induce stresses if the member is unrestrained when it is heated (Figures 1a and 1b). However, in fully restrained members stress occurs without strain (Figures 1d and 1e).

When a body is subjected to a nonuniform temperature gradient, irregular volume changes are produced. Thermal stresses arise because thermal expansion is restricted within the body. A similar body with a uniform or linear change in temperature undergoes free thermal expansion, and stresses are not developed.

As a consequence of a nonlinear temperature gradient, a set of self-equilibriating stresses develop throughout the depth of the section. These stresses result from induced internal strains developed to prevent the distortion of the plane section as a result of a nonlinear temperature distribution. Thus the nonlinear strain distribution caused by thermal effects plus a nonlinear strain distribution caused by the self-equilibriating stresses combine to satisfy the assumption of a total linear strain gradient. The self-equilibriating stresses are similar in form to the residual stresses present in rolled steel sections as a result of cooling and will be referred to as eigenstresses. Eigenstresses depend on the nonuniform deformation resulting from thermal effects and are independent of the boundary or support conditions of a structure.

If a simply supported beam under the influence of a nonuniform temperature gradient is allowed to deform freely (Figure 1c), then eigenstresses will be developed in the longitudinal direction. The beam also will assume an upward curvature. When the member is restrained, bending stresses are induced. This is shown in Figure 1d where axial expansion caused by an increase in mean temperature is allowed but where end rotation is restrained. The resulting bending stress adds to the eigenstress to give total thermal stress.

If the member is restrained axially (Figure 1e), then axial stress will be induced and mean temperature will change. Eigenstress, bending stress, and axial stress contribute to total longitudinal thermal stress in the member shown in Figure 1e where the ends are rigidly fixed.

Stresses arising from a restraint to axial or rotational movement are functions of the boundary conditions of the member. Eigenstresses are not a function of these boundary conditions but are directly related to vertical temperature distribution.

A summary of the effects of various vertical temperature gradients on both simply supported and continuous members is shown in Figure 1. Figure 1f illustrates the effect of a nonlinear vertical temperature gradient on the response of a 2-span continuous beam. Eigenstresses resulting from the nonlinear gradient are induced throughout the length of the beam. The gradient causes an upward positive curvature, and continuity stresses develop (3). The positive gradient shown is associated with summer daytime conditions. As a result of heating during a winter day, negative temperature gradients can develop as heat is lost from the surface of the structure during the evening. Figure 1f shows a typical summer daytime state. A winter state would be shown by reversing the stresses shown in the figure.

CONSEQUENCES OF THERMAL LOADING

In current bridge design practice, expansion devices are used to accommodate longitudinal thermal movements. Thermal stresses resulting from temperature gradients, however, generally are ignored. Observations indicate that thermal loading can seriously affect the serviceability as well as the structural integrity of a bridge structure (3, 4).

Hilton (5) has reported thermally induced vertical movements of simply supported steel bridge girders that have occurred before the concrete deck has been placed. An upward deflection of 0.40 in. (1 cm) was not uncommon on sunny days for a span length of 42.5 ft (13 m). A deflection of this magnitude can affect the final thickness of the

deck slab. Hilton (5) also found that the deflection of each girder was a function of its orientation to the sun and changed as the position of the sun changed.

Major stress-inducing effects caused by thermal loading occur in continuous structures. In a continuous bridge beam, a temperature rise at the upper surface produces positive flexural moments, which causes tensile stresses on the lower surface. Leonhardt and Lippoth (3) have reported crack damage caused by this type of thermal stress in 2-span continuous beams in the vicinity of the intermediate supports. This type of behavior and associated damage also have been observed in exposed building structures (6, 7).

A temperature difference between the top and bottom of a box-girder bridge also can result in thermally induced transverse bending and axial stresses (Figure 2) (4). With strong and prolonged solar radiation on the surface of a box-girder bridge, the interior air temperature increases and may exceed 100 F (38 C) (3). When the outer air cools during the night, a temperature difference between the interior and exterior of the box develops. For a temperature difference of 27 F (-2.8 C) between the outer and inner surfaces of a hollow box, transverse tensile stresses of 500 lb/in.^{2} (3500 kPa) are possible (3).

Damage to the abutments of an intermediate support line of a continuous, precast, prestressed bridge has been reported by Monnier (8). When heated, precast beams tend to "hog" upward (Figure 3) (8). If continuity reinforcement is absent at the bottom of the beams, horizontal prying forces that develop as a result of temperature change, creep, and shrinkage may cause damage (9, 10).

SOURCES OF HEAT

An exposed concrete bridge deck is heated or cooled by the following:

1. Convection to or from the surrounding atmosphere,
2. Radiation from the sun, and
3. Radiation to or from the sky or surrounding objects.

These sources are shown in Figure 4. Temperature changes induced by these sources depend on a number of factors such as:

1. Latitude of locality,
2. Orientation of bridge deck to the sun,
3. Time of day and season,
4. Degree of cloudiness and relative humidity,
5. Nature and color of bridge deck surface, and
6. Thermal properties of constituent materials of the bridge.

The maximum intensity of solar radiation occurs in the summer and generally increases with increasing proximity to the equator. Available data indicate a maximum intensity of incoming solar radiation on a horizontal surface between 11:00 a.m. and 2:00 p.m. (11, 12).

Radiant energy from the sun is partially reflected and partially absorbed. Reflected energy does not influence bridge temperature. Absorbed energy, however, heats the bridge deck surface and gives rise to a temperature gradient through the deck. Some of the absorbed radiant energy is lost from the surface by convection and reradiation (Figure 4). The radiation absorbed by a bridge deck is a function of the nature and color of the surface (absorptivity). A dark, rough surface has higher absorptivity than does a light, smooth surface and consequently absorbs more solar radiation.

The amount of radiant energy absorbed by the bridge deck from the atmosphere depends on the relative humidity of the air. This heat gain is often offset by the heat reradiated back into the atmosphere. Expressions for determining the heat radiated by and absorbed by a horizontal surface facing the sky are available (13).

Convective heat transfer from atmosphere to bridge deck is a function of wind

Figure 1. Effects of various temperature gradients.

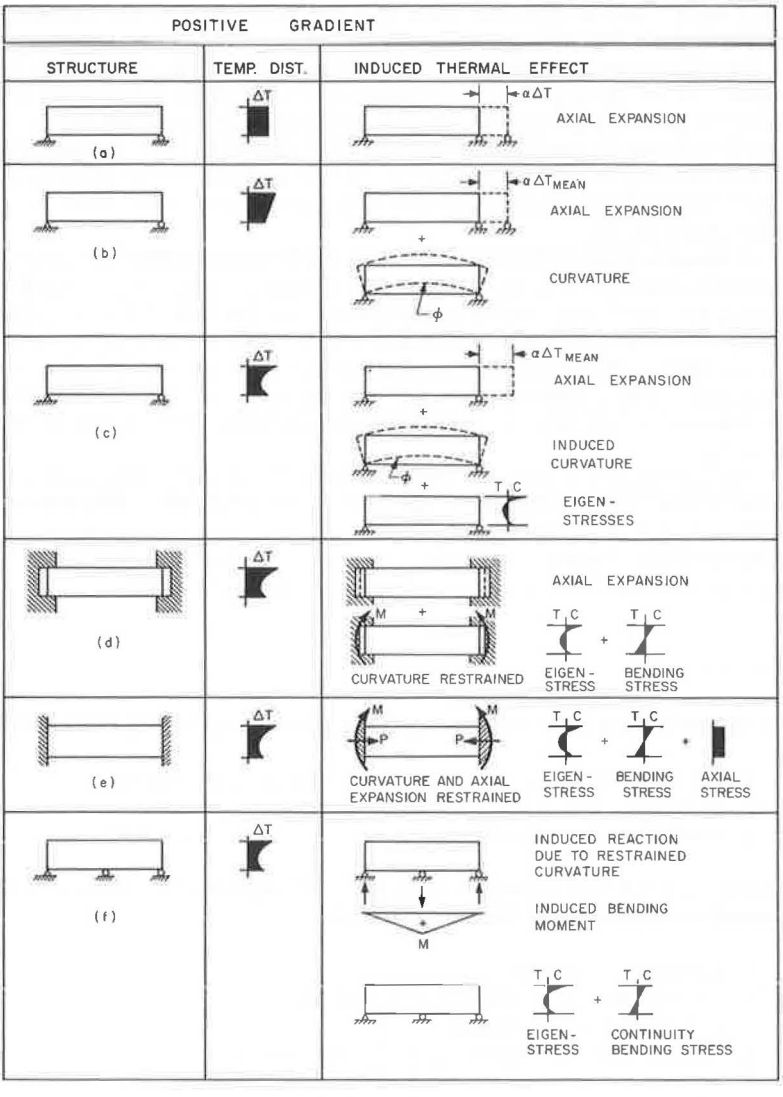

Figure 2. (a) Axial stresses caused by transverse elongation of deck slab and (b) bending stresses caused by restraint of transverse "hogging" in box girders.

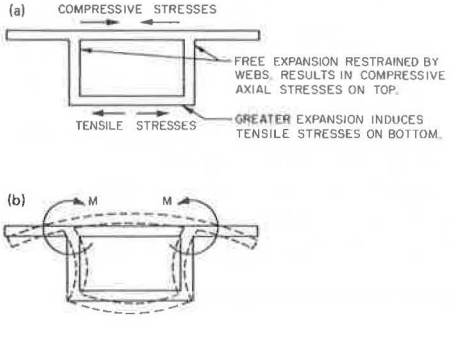

Figure 3. Support prying forces.

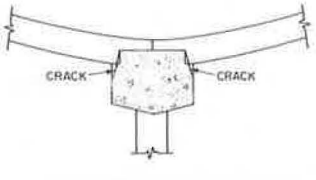

THERMALLY INDUCED CURVATURE RESULTS IN PRYING FORCES

velocity, ambient air temperature, and deck surface temperature. The variation of both wind velocity and air temperature with time makes it difficult to predict heat gained by convection. By considering monthly average values of wind velocity and temperature, one can develop average values of heat transfer surface coefficients (14).

BRIDGE TEMPERATURES

Vertical temperature distribution through a concrete section depends on local weather conditions, section depth, and thermal properties of the concrete. The basic quantities that determine the thermal behavior of concrete are thermal conductivity, thermal diffusivity, specific heat, and coefficient of thermal expansion. These properties vary widely for typical concretes and are a function of composition of the mix, degree of saturation, and mineralogical character of the aggregate used (15, 16). An analysis of heat flow includes the following values for the concrete properties: 0.8 Btu·ft/ft^2·h·F (1.4 W/m·C), 0.02 ft^2/h (0.002 m^2/h), 0.23 Btu/lb·F (960 J/kg·C), and 6×10^{-6}/F (11×10^{-6}/C) for conductivity, diffusivity, specific heat, and coefficient of thermal expansion respectively. These values are typical for exposed concrete of normal weight.

Prediction of temperature effects on a structure from records of air temperature and solar radiation is important to design engineers. By interpreting regularly recorded weather data, they can make suitable provisions in design to resist or allow for movements and stresses induced by temperature changes. Both Barber (17) and Zuk (18) have been able to relate local weather data to maximum observed surface temperatures in bituminous and concrete pavements and bridge decks.

Analysis of temperature distribution throughout the depth of a section of a typical structure is complex because temperature varies with time, position in the section, and from section to section. Results to be presented are based on an analysis of 1-directional heat flow from the upper and lower surfaces of a unit strip taken from a wide beam or slab bridge deck. Included in the analysis are the following assumptions:

1. The member is homogeneous;
2. Surface heat transfer coefficients remain constant throughout the analysis time period; and
3. Thermal properties of the member are independent of temperature variation.

The 1-directional heat flow leads to a partial differential equation that was solved by using the finite difference method. The resulting iterative solution is similar to solutions developed by Emerson (19) and Krishnamurthy (20). When shade temperature, solar radiation, and wind at the exposed surfaces are known for a given day, then the temperature-time variation within a section can be obtained. Comparisons of measured and computed winter and summer gradients show good agreement (19). Because of the wide variation in climatic conditions in any given locality, a variety of temperature distributions is possible. Several such distributions have been observed or suggested on the basis of observed data. Included in these distributions are:

1. A linear temperature distribution in the top slab of a box section (21),
2. A constant temperature in the top slab of a box section (4), and
3. A distribution approximated by a sixth-degree parabola applicable to deep sections (4, 19).

The temperature distribution used in the third item has the form

$$t_y = \frac{Ty^6}{d^6} \qquad (1)$$

where

t_y = temperature at fiber in question,
y = vertical distance from bottom of section to fiber in question,
d = depth of section, and
T = maximum temperature differential in the section.

A series of temperature distributions corresponding to the maximum temperature gradient was computed for rectangular concrete sections of different depths. The calculations were based on the values for conductivity, specific heat, and diffusivity previously mentioned. Values of solar radiation and ambient air temperature observed in Toronto, Ontario, on May 31, 1973, a day of high-intensity solar radiation and higher than average temperature range, were used in the analysis (Figure 5). Values of average solar radiation for the May to July period are similar for the United States and southern Canada. Hence the data shown in Figure 5 are representative.

The results of the analyses of the distributions are shown in Figure 6. It is apparent that temperature distribution is a function of section depth. For the shallowest section, temperature distribution is linear, and a temperature gradient of approximately 23 F (-5 C) exists. As section depth increases, surface temperature increases and appears to reach a maximum for sections greater than 30 in. (76 cm) in depth. Temperature distribution appears to be nonlinear for depths greater than 12 in. (30 cm), and temperature difference between upper and lower surfaces increases up to a section depth of 30 in. (76 cm) and remains constant for section depths greater than this. The central portion of the deeper sections does not appear to be affected by the diurnal heating cycle. A maximum temperature differential of 34 F (1.1 C) between the interior and the top surface appears to be typical for the deeper sections. Figure 6 also shows the temperature distribution corresponding to a sixth-degree parabola (equation 1). For sections greater than 24 in. (61 cm) deep the correlation between gradients calculated by using the heat transfer analysis and those predicted by a sixth-degree parabola is very good. However, for the 7-in. (18-cm) section, the correlation is poor.

Asphalt has a higher absorptivity than a normal gray-white concrete deck, and the surface temperature of a deck with asphalt will be different from that of a concrete deck without asphalt under similar climatic conditions. The computations were repeated for a concrete deck with a 2-in. (5-cm) asphalt covering. The temperature of the concrete below the asphalt was 6.3 F (-14.2 C) lower than that for an exposed deck. These results support the suggestion that a 1.5- to 2-in. (4- to 5-cm) thickness of surfacing is required before the insulation value of asphalt surfacing compensates for the greater heat absorption associated with dark surfaces (22).

In continuous structures, thermally induced curvatures result in continuity stresses. Maximum curvature occurs at the same time of day as maximum temperature gradient (12:00 noon to 1:00 p.m. for thin members and 3:00 p.m. to 4:00 p.m. for thicker sections). Thin sections developed larger curvatures than did thick sections (Figure 7). Continuity thermal stresses are a function of both curvature and member depth. The maximum continuity stress in a multispan continuous system is given by the following equation:

$$\sigma = C_1 C_2 E \phi d \qquad (2)$$

where

σ = bending stress resulting from continuity,
C_1 = a constant that is a function of number of spans (C_1 = 1.5 for 2-span system, C_1 = 1.0 for a multispan system)(3),
C_2 = a constant that is a function of section geometry (C_2 = 0.5 for rectangular member),
E = Young's modulus [taken as 5×10^6 lb/in.^{2} (34.5×10^6 kPa)],

Figure 4. Heat flow in exposed bridge deck.

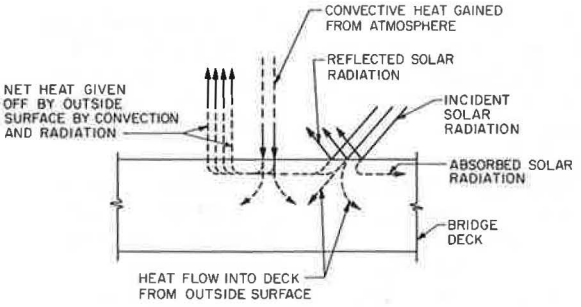

Figure 5. Intensity of solar radiation and range in ambient air temperature.

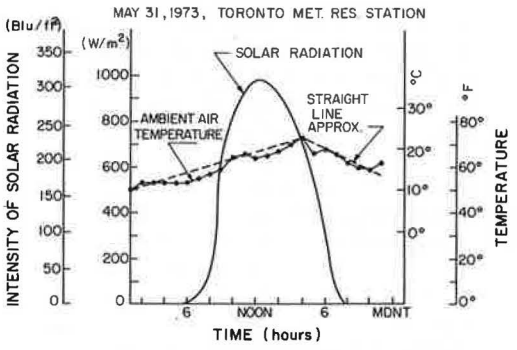

Figure 6. (a) Temperature distribution, (b) stress distribution corresponding to calculated gradient, and (c) stress distribution corresponding to sixth-order parabola for various section depths.

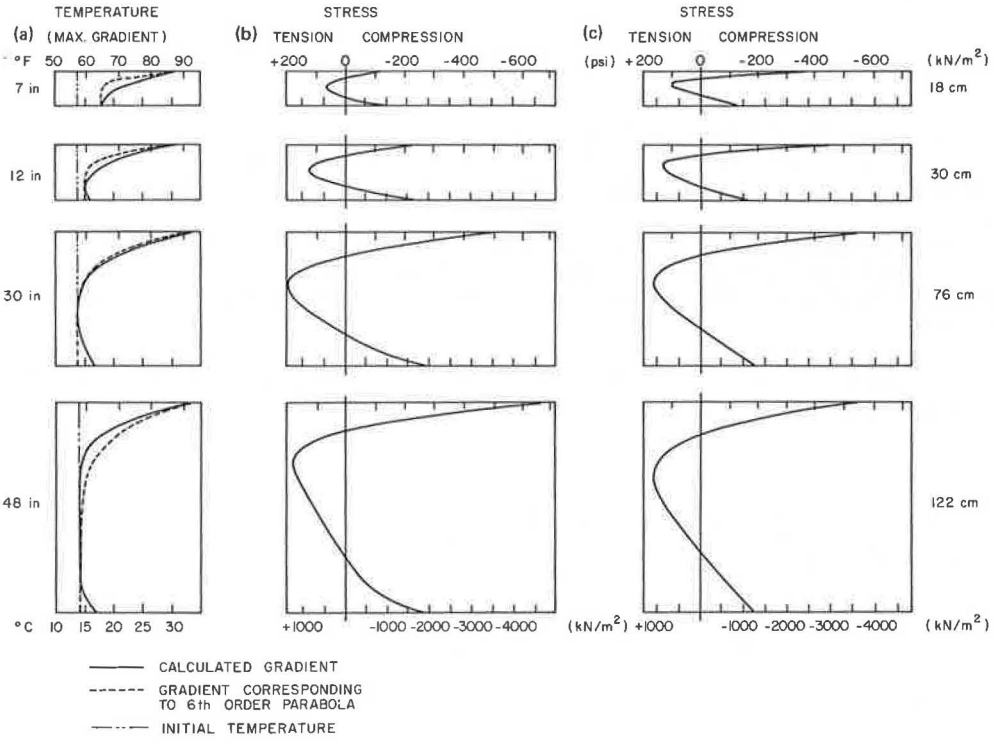

ϕ = curvature, and
d = member depth.

Thus continuity stresses are proportional to ϕd for a given material and span geometry. Figure 8 shows the relationship between nondimensional curvature and depth for both surfaced and unsurfaced members. The figure indicates that for rectangular members maximum continuity stresses occur in members that are approximately 15 in. (38 cm) deep. Figure 9 shows the influence of member depth on mean bridge temperatures for both surfaced and unsurfaced conditions. The difference between shallow and deep members exists because of the moderating influence of the interior of deeper slabs on temperature change. The computed maximum mean temperature and, therefore, maximum elongation occur between 6:00 p.m. and 7:00 p.m. for both shallow and deep slabs. This agrees with measurements of mean bridge temperature (19, 23).

Figure 10 shows the relationship between mean temperature and shade temperature for various depths. Mean temperature is higher than ambient shade temperature for sections thinner than 20 in. (51 cm). For thicker sections [>36 in. (92 cm)], the ratio of mean temperature to shade temperature appears to approach a constant value. Hence, if maximum shade temperature is known, mean temperature of a section of given depth under known climatic conditions can be estimated with reasonable accuracy.

THERMAL STRESSES

The analysis used in the prediction of stress is based on 1-dimensional beam theory and includes the following assumptions:

1. The material is homogeneous and isotropic;
2. Plane sections remain plane after bending is valid (Euler-Bernoulli assumption);
3. Temperature varies with depth, but transverse or longitudinal temperature variations do not exist;
4. Thermal stresses can be considered independently of stress or strain imposed by other loading conditions (principle of superposition applies); and
5. The section analyzed is far enough from a free end for end-distortion effects to be insignificant.

The resultant expression for longitudinal eigenstress, σ_z, at a distance above the neutral axis, has the following form (4, 23, 24):

$$\sigma_z = E\alpha \left[-\Delta T + x \frac{\int_{x_1}^{x_2} \bar{y} x \Delta T dx}{\int_{x_1}^{x_2} \bar{y} x^2 dx} + \frac{\int_{x_1}^{x_2} \bar{y} \Delta T dx}{\int_{x_1}^{x_2} \bar{y} dx} \right] \quad (3)$$

where

α = coefficient of thermal expansion,
x_1, x_2 = distance from neutral axis to extreme fibers,
$\bar{y}$ = total section width excluding voids,
x = distance from neutral axis to fiber in question,
ΔT = change in temperature, and
dx = thickness of elemental particle.

This expression applies to a long, thin member with no end restraints. If the second term in equation 3 is omitted, then the member has restraining moments at the ends

gure 7. Maximum curvature versus depth.

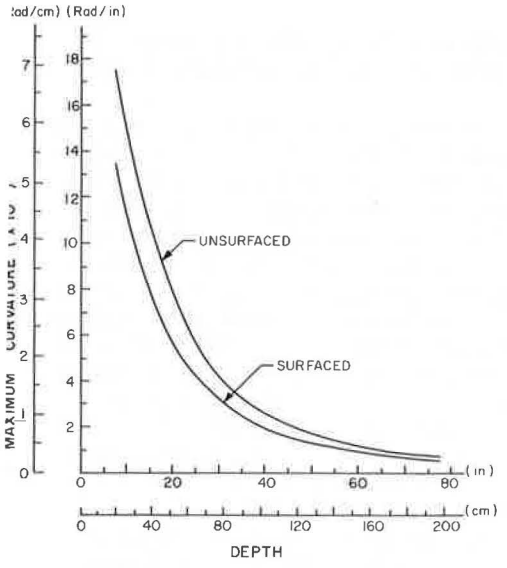

Figure 8. Curvature x depth versus depth.

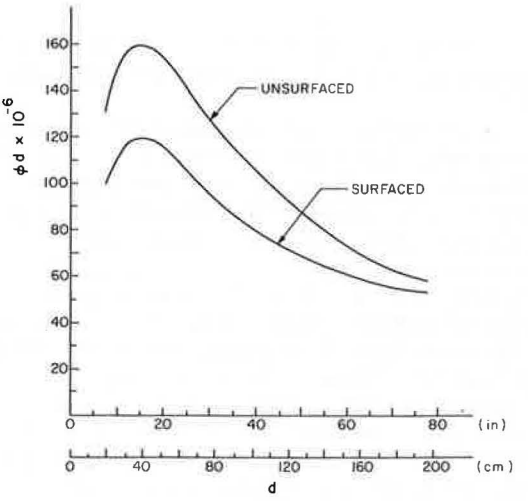

igure 9. Maximum mean bridge temperature versus epth.

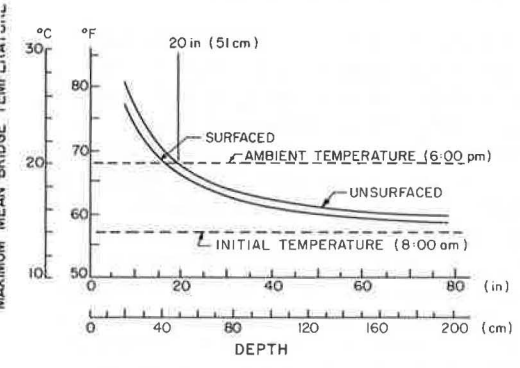

Figure 10. Ratio of mean temperature to shade temperature versus depth.

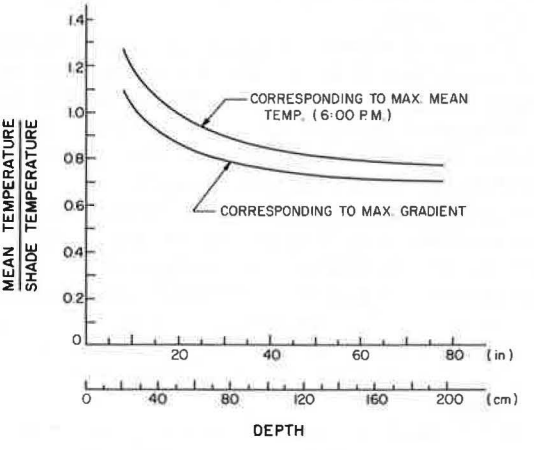

igure 11. Maximum surface and interior stresses.

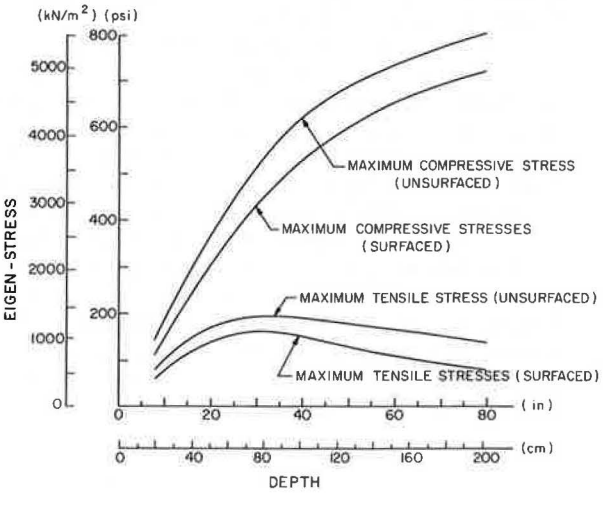

only. If the third term is omitted, then a restraining axial force only is present. If both the second and third terms are omitted, then the ends of the member are rigidly held.

Figure 6b shows the eigenstresses produced by the temperature gradients discussed previously. The stress distributions are characteristic of those produced by a positive temperature gradient. Compressive stresses are present in the upper and lower surfaces; tensile stresses are present in the central region of the section. As section depth increases, maximum compressive surface stress also increases; maximum interior tensile stress reaches a maximum at a depth of approximately 30 in. (76 cm). A summary of maximum stresses is shown in Figure 11 for both a surfaced and unsurfaced section. Adding 2 in. (5 cm) of asphalt lowers maximum stress levels slightly.

Stress values of more than 700-lb/in.^{2} (4800-kPa) compression were obtained on the top surface of some of the deeper sections. In prestressed members, where sustained compressive stress is present, the additional stress of 700 lb/in.^{2} (4800 kPa) corresponds to approximately 45 percent of an acceptable allowable stress [1,600 lb/in.^{2} (11 000 kPa)]. Combined longitudinal compressive stresses caused by live load, dead load, prestress, and thermal load reduce flexural tensile strength of concrete in the transverse direction (25).

A major stress-inducing effect of thermal loading in bridges occurs in continuous structures where interior supports offer restraint. To minimize the effects of dead load, many engineers construct new bridges that are cellular (that is, they include voided slabs, box girders, and T-beams). The magnitude of eigenstress is affected by web thickness in both box sections and T-sections. An increase in the ratio of web thickness to flange thickness results in an increase in maximum compressive stress and a decrease in maximum tensile stress (Figure 12). This trend is more pronounced in deep sections.

Figure 13 shows the influence of web thickness on induced curvature and indicates that curvature is insensitive to a change in web thickness. Similar results were obtained from various thermal stress analyses of T-sections with varying web thicknesses.

Although thermal stress caused by temperature gradients is generally ignored in design, Bosshart (26) has shown that stresses caused by thermal effects can be a large percentage of the total stress in continuous spans. Observations have indicated that, on a warm, sunny day, vertical temperature differences of 40 F (4.4 C) are possible. This temperature variation is considerably larger than variations specified in codes containing clauses dealing with temperature gradients (27). Temperature differences of this magnitude give rise to thermal stresses on the bottom fiber at a mid-span section that were equal in magnitude to maximum design live load stress and top fiber stresses that were 3 times as large as the stresses produced by maximum live load. Thermal stresses as high as 780 lb/in.^{2} (5400 kPa) were computed from observed temperature data (26).

Analysis of a continuous member under thermal gradient consists of predicting the magnitude of eigenstresses (equation 3) and continuity stresses (equation 2). For a given structure, one can use the data shown in Figures 7 and 12 to predict both continuity and eigenstresses.

Two typical, prestressed, concrete bridge structures were analyzed under thermal loading by using the solar radiation and ambient air temperature data shown in Figure 5. The structures chosen were a 2-span, prestressed, box-girder bridge with a section depth of 78 in. (198 cm) and a 3-span, prestressed, voided-slab bridge with a maximum depth of 52 in. (132 cm). The box-girder bridge is typical of box structures used in California. Typical stress values for dead and live load were available (28). The voided-slab bridge is representative of bridge structures used in Ontario. Values of stress caused by dead and live load were computed.

Eigenstresses for both box-girder and voided-slab bridges can be obtained from the data shown in Figure 12. Both the box-girder and voided-slab bridges were analyzed by considering equivalent I-sections, each of which had a different web thickness and depth. Induced curvature is insensitive to web thickness. Therefore, Figure 7, which is based on a rectangular section, can be used to obtain maximum curvature and continuity stresses.

Figure 12. Influence of web thickness on eigenstress.

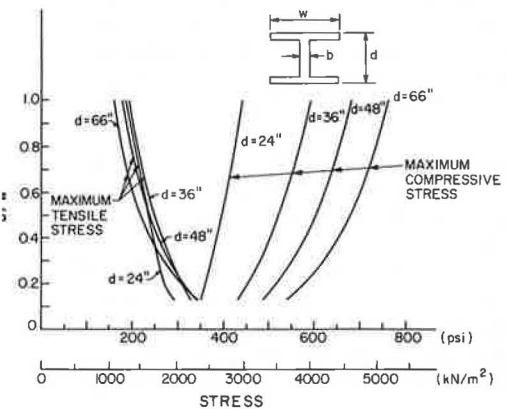

Figure 13. Influence of web thickness on curvature.

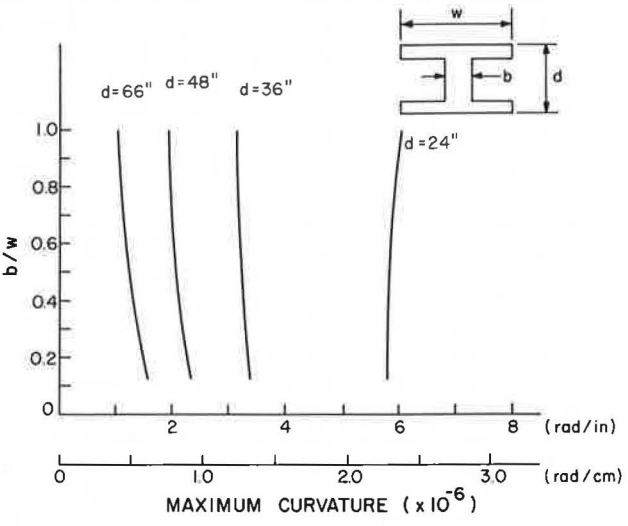

Figure 14. (a) Bending moment caused by thermal load, (b) total thermal stress, and (c) live load and impact stress in a box-girder bridge.

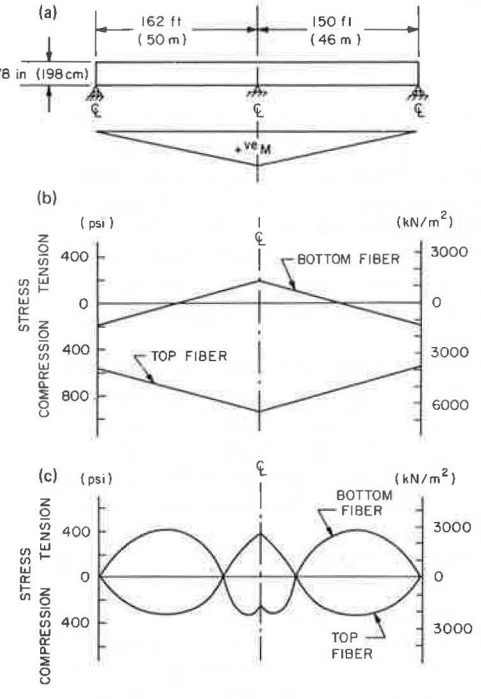

Figure 15. (a) Bending moment caused by thermal load, (b) total thermal stress, and (c) live load and impact stress in a voided-slab bridge.

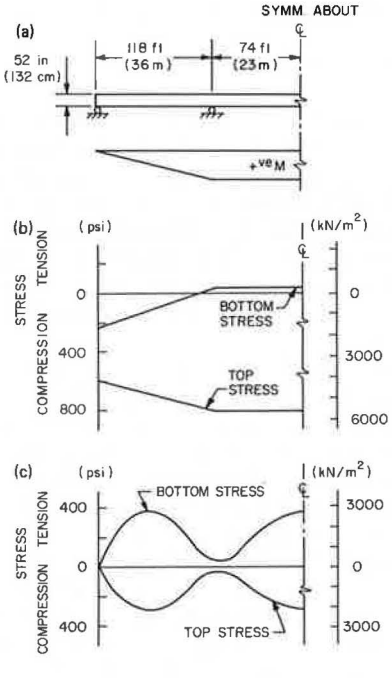

Figures 14 and 15 show the results of thermal stress analyses for the box-girder and the voided-slab bridges respectively. Figure 14b shows total thermal stress. Maximum thermally induced stress for the 2-span structure occurs on the top fiber at the intermediate support. Compressive stresses of 940 lb/in.^{2} (6500 kPa) are predicted. The entire top surface of the structure is in compression; average compressive stress is 770 lb/in.^{2} (5300 kPa), and this is due to thermal effects alone. Half of the bottom surface is subjected to tension; stresses are 200 lb/in.^{2} (1400 kPa) at the intermediate support.

Figure 14c shows the stresses caused by live load plus impact load. The stresses due to thermal effects are almost 2.5 times as large as those caused by live load plus impact at the mid-span section. They are greater than those caused by live load plus impact at every point on the top surface of the bridge.

The total design compressive stresses on the top surface are increased by 50 percent by the addition of thermal effects. This increase is from a maximum of 1,400 lb/in.^{2} (9700 kPa) to 2,100 lb/in.^{2} (14 500 kPa) at the mid-span sections. Stresses caused by thermal load, therefore, represent 33 percent of the total stress at the top fiber. At the bottom surface thermal stresses and stresses caused by gravity loads tend to cancel each other.

Figures 15b and 15c show respectively total thermal stress and live load plus impact stresses for the 3-span, voided-slab bridge. Top compressive stresses caused by thermal load are almost 3 times as large as those caused by maximum live load. Average compressive stresses of 715 lb/in.^{2} (4900 kPa) caused by thermal effects alone were obtained on the top surface; the entire center span was subjected to stresses of more than 800 lb/in.^{2} (5500 kPa). Bottom stresses were much smaller. Tensile stresses of only 40 lb/in.^{2} (280 kPa) were obtained on the bottom surface throughout the entire center span. Adding thermal stress increased total working top stress values by more than 47 percent. Total top fiber compressive stresses of more than 2,400 lb/in.^{2} (16 500 kPa) were obtained.

DISCUSSION OF FINDINGS

The strains introduced into concrete bridge structures as a result of a summer diurnal heating cycle are similar in magnitude to those associated with lifetime shrinkage strains. Similarly, stresses resulting from restraint of thermal strains can exceed those associated with design live load and can have a different sign. Solar heating or cooling introduces nonlinear temperature gradients in concrete structures. Hence expansion or contraction, which results from changes in the mean temperature, and bending, which develops as a consequence of the nonlinear gradient, should be considered in design. Current design practice appears to consider the influence of mean temperature only.

Analyses of rectangular, T-, and I-sections of various depths indicate that temperature distribution, stress distribution, maximum curvature, and maximum mean bridge temperature resulting from a typical diurnal heating cycle depend on section depth. Shallow sections generally exhibit larger curvatures and higher mean temperatures than deeper sections do. For deeper sections, the moderating influence of the interior where temperatures do not change appreciably during a daily heating cycle results in high self-equilibriating stresses and low curvature.

A detailed analysis of the stresses induced in various continuous concrete structures of various cross sections and depths indicates that surface compressive stresses of more than 900 lb/in.^{2} (6200 kPa) and interior tensile stresses of more than 300 lb/in.^{2} (2100 kPa) are possible on a typical hot summer day in a typical continuous concrete structure [48 in. (122 cm) in depth]. Local total thermal stresses several times larger than stresses caused by live load were computed. Consideration of thermal stress substantially increased (by 50 percent) total design stress and accounted for a third of total working stress. Typical reported thermal and elastic properties were assumed for the concrete in the 1-dimensional heat-flow analysis. The stresses previously noted show a sign change for winter conditions and have a magnitude of approximately 70 to 80 percent of the summer values.

The stresses developed as a consequence of heating and cooling cycles can affect the serviceability of concrete structures, particularly the deck slab in deep, solid-concrete structures and both deck slab and webs in cellular, box-type structures. The stress range caused by thermal effects plus gravity and prestressing loads and computed for 2 examples was found to exceed 40 percent of the allowable compressive design stress for these structures.

Thermal stresses caused by daily heating and cooling should be considered in conjunction with lifetime creep and shrinkage stresses and heat of hydration stresses. All these stress effects may contribute to the lack of serviceability of an exposed structure.

CONCLUSIONS

As a consequence of the relatively poor thermal conductivity of concrete, significant flexural stresses develop in concrete bridge superstructures when they are subjected to solar heating or cooling and changes in ambient temperature. These thermally induced flexural stresses can exceed 40 percent of the allowable compressive stress for concrete. Although they do not influence the strength of the superstructure, they can affect long-term serviceability.

Current design procedures should be considered adequate provided that reinforcing is well distributed throughout a concrete superstructure. Calculation procedures that consider stress-inducing thermal effects should be used to proportion the reinforcement.

ACKNOWLEDGMENTS

This research was carried out with the support of the Transportation Development Agency Canada in the form of a graduate fellowship awarded to Radolli. The research also was aided by the National Research Council of Canada and the Department of Civil Engineering, University of Waterloo. This support is gratefully acknowledged.

REFERENCES

1. J. C. Reynolds and J. H. Emanuel. Thermal Stresses and Movements in Bridges. Journal of Structural Division, Proc., American Society of Civil Engineers, Vol. 100, No. ST1, Jan. 1974, pp. 63-78.
2. Standard Specifications for Highway Bridges. American Association of State Highway Officials, 1973.
3. F. Leonhardt and W. Lippoth. Folgerungen aus Schaden an Spannbetonbrücken. Beton-und Stahlbetonbau, Heft 10, Vol. 65, Oct. 1970, pp. 231-244.
4. M. J. N. Priestley. Effects of Transverse Temperature Gradients on Bridges. Central Laboratories, New Zealand Ministry of Works, Rept. 394, Oct. 1971.
5. M. H. Hilton. Factors Affecting Girder Deflections During Bridge Deck Construction. Highway Research Record 400, 1972, pp. 55-68.
6. A. R. Meenan. Parking Garages for New Orleans Superdome. Journal of Prestressed Concrete Institute, Vol. 19, No. 2, March-April 1974, pp. 98-111.
7. J. N. Deserio. Thermal and Shrinkage Stresses—They Damage Structures! American Concrete Institute Publication SP27, 1971, pp. 43-49.
8. T. Monnier. Cases of Damage to Prestressed Concrete. HERON, Vol. 18, No. 2, 1972.
9. L. Zetlin, C. H. Thorton, and I. P. Lew. Design of Concrete Structures for Creep, Shrinkage and Temperature Changes. Symposium, Design of Concrete Structures for Creep, Shrinkage, and Temperature Changes, International Association for Bridge and Structural Engineering, Final Rept., Vol. 5, Zurich, Switzerland, 1970.
10. Handbook on the Unified Code for Structural Concrete. Cement and Concrete Association, London, England, CP110:1972, pp. 94-96.

11. F. H. Faust, L. Levine, and F. O. Urban. A Rational Heat Gain Method for the Determination of Air Conditioning Cooling Loads. Trans., American Society of Heating and Ventilating Engineers, Vol. 41, 1935.
12. Monthly Radiation Summary. Atmospheric Environment Service, Canada Ministry of the Environment, Information Canada, Ottawa, 1973.
13. J. S. Alford, J. E. Ryan, and F. O. Urban. Effect of Heat Storage and Variation in Outdoor Temperature and Solar Intensity on Heat Transfer Through Walls. Trans., American Society of Heating and Ventilating Engineers, Vol. 45, 1939, pp. 369-396.
14. M. W. R. Capps. The Thermal Behavior of the Beachley Viaduct/Wye Bridge. U. K. Road Research Laboratory, Crowthorne, Berkshire, England, Rept. LR234, 1968.
15. A. M. Neville. Properties of Concrete. Pitman Publishing Corp., New York, 1972, pp. 428-438.
16. D. G. R. Bonnel and F. C. Harper. The Thermal Expansion of Concrete. National Building Studies, Her Majesty's Stationery Office, London, England, Technical Paper 7, 1951.
17. E. S. Barber. Calculation of Maximum Pavement Temperature From Weather Reports. HRB Bulletin 168, 1957, pp. 1-8.
18. W. Zuk. Thermal Behavior of Composite Bridges—Insulated and Uninsulated. Highway Research Record 76, 1965, pp. 231-253.
19. M. Emerson. The Calculation of the Distribution of Temperature in Bridges. U. K. Transport and Road Research Laboratory, Crowthorne, Berkshire, England, Rept. LR561, 1973.
20. N. Krishnamurthy. Temperature Effects on Continuous Reinforced Concrete Bridge. Alabama Highway Department, Highway Planning and Research Rept. 58, Research Project 930-047, July 1971.
21. D. R. H. Maher. The Effects of Differential Temperature on Continuous Prestressed Concrete Bridges. Civil Engineering Transactions, Institution of Engineers, Australia, Vol. CE12, No. 1, Paper 273, April 1970, pp. 29-32.
22. A. W. Hendry and J. K. Page. Thermal Movements and Stresses in Concrete Slabs in Relation to Tropical Conditions. International Symposium on Concrete and Reinforced Concrete, Réunion Internationale des Laboratoires d'Essais et de Recherches sur les Materiaux et les Constructions, Part 2, July 1960, pp. 1-26.
23. W. I. J. Price and R. G. Tyler. Effect of Creep, Shrinkage and Temperature on Highway Bridges in the United Kingdom. Symposium, Design of Concrete Structures for Creep, Shrinkage, and Temperature Changes, International Association for Bridge and Structural Engineering, Final Rept., Vol. 6, Zurich, Switzerland, 1970, pp. 81-93.
24. R. Hoyle. Plane Strain and Plane Stress. In Thermal Stress, Sir Isaac Pitman and Sons Ltd., London, England, 1964, pp. 43-51.
25. G. Winter and A. H. Nilson. Design of Concrete Structures. McGraw-Hill Book Co., New York, 8th Ed., 1972.
26. H. Bosshart. Temperaturspannungen in Spannbetonbrücken. Symposium, Design of Concrete Structures for Creep, Shrinkage, and Temperature Changes, International Association for Bridge and Structural Engineering, Vol. 6, Zurich, Switzerland, 1970, pp. 73-80.
27. D. J. Lee. The Theory and Practice of Bearings and Expansion Joints for Bridges. Cement and Concrete Association, London, England, 1971.
28. Manual of Bridge Design Practice. California Department of Transportation, Section 7, 1971.